Protection against hemorrhagic shock in mice genetically deficient in poly(ADP-ribose)polymerase

Lucas Liaudet*†, Francisco Garcia Soriano‡§, Éva Szabó¶, László Virág¶, Jon G. Mabley¶, Andrew L. Salzman*¶, and Csaba Szabó‡¶‖

¶Inotek Corporation, Suite 419 E, 100 Cummings Center, Beverly, MA 01915; *Division of Pulmonary Medicine, Allergy and Clinical Immunology, Department of Pediatrics, Children's Hospital Medical Center, 3333 Burnet Avenue, Cincinnati, OH 45229; and ‡Department of Surgery, New Jersey Medical School, University of Medicine and Dentistry of New Jersey, Newark, NJ 01703

Edited by Solomon H. Snyder, Johns Hopkins University School of Medicine, Baltimore, MD, and approved June 21, 2000 (received for review May 18, 2000)

Hemorrhagic shock (HS) and resuscitation leads to widespread production of oxidant species. Activation of the enzyme poly(ADP-ribose) polymerase (PARP) has been shown to contribute to cell necrosis and organ failure in various disease conditions associated with oxidative stress. We tested the hypothesis whether PARP activation plays a role in the multiple organ dysfunction complicating HS and resuscitation in a murine model of HS and resuscitation by using mice genetically deficient in PARP ($PARP^{-/-}$) and their wild-type littermates ($PARP^{+/+}$). Animals were bled to a mean blood pressure of 45 mmHg (1 mmHg = 133 Pa) and resuscitated after 45 min with isotonic saline (2× volume of shed blood). There was a massive activation of PARP, detected by poly(ADP-ribose) immunohistochemistry, which localized to the areas of the most severe intestinal injury, i.e., the necrotic epithelial cells at the tip of the intestinal villi, and colocalized with tyrosine nitration, an index of peroxynitrite generation. Intestinal PARP activation resulted in gut hyperpermeability, which developed in $PARP^{+/+}$ but not $PARP^{-/-}$ mice. $PARP^{-/-}$ mice were also protected from the rapid decrease in blood pressure after resuscitation and showed an increased survival time, as well as reduced lung neutrophil sequestration. The beneficial effects of PARP suppression were not related to a modulation of the NO pathway nor to a modulation of signaling through IL-6, which similarly increased in both $PARP^{+/+}$ and $PARP^{-/-}$ mice exposed to HS. We propose that PARP activation and associated cell injury (necrosis) plays a crucial role in the intestinal injury, cardiovascular failure, and multiple organ damage associated with resuscitated HS.

gut | knockout

Hemorrhagic shock (HS) and resuscitation trigger the expression of a cascade of inflammatory mediators, resulting in tissue damage, multiple organ dysfunction, and eventually death. Regional hypoxia associated with hemorrhage and oxidative stress during resuscitation contribute to the development of this systemic inflammatory response (1). In recent years, evidence has accumulated that an important mechanism of tissue injury during oxidative stress was the activation of PARP [also termed poly(ADP-ribose) (PAR) synthetase or PARS], an enzyme abundantly present in the nucleus of eukaryotic cells (2). Activation of PARP is triggered by oxidant-mediated DNA single-strand breaks and initiates an energy-consuming futile intracellular cycle, leading to the rapid depletion of the cellular stores of NAD^+ (the substrate of PARP) and ATP, resulting in cell dysfunction and necrotic-type cell death (3, 4). DNA single-strand breakage, PARP activation, and cell death have been demonstrated *in vitro* in cells exposed to various oxygen-centered free radicals (2), as well as to peroxynitrite, a reactive nitrogen species formed from the rapid reaction of NO with superoxide radical (5). *In vivo*, PARP activation has also been convincingly shown to act as a common effector of oxidant-dependant damage in various pathophysiological conditions including ischemia-reperfusion injury (6, 7), localized inflammation (8), and endotoxic shock (9).

It is well established that HS is associated with the formation of free radicals and oxidant species. In particular, recent data have indicated that peroxynitrite formation occurred in the early phase of resuscitated HS, the source of NO being here the constitutive isoforms of NO synthase (10). Also, DNA injury has been detected in tissues obtained from animals subjected to HS (11). These observations indicate that all of the conditions required for PARP activation are present in HS. Previous studies testing pharmacological inhibitors of PARP in experimental HS suffered from problems with the limited selectivity of the inhibitor for PARP and their relatively low potency (12, 13). In the present study, we have investigated in more detail the potential role PARP activation may play in HS by using genetically engineered animals lacking the PARP gene. In this respect, the data reported herein provide more definitive and mechanistic information than what can be given by a purely pharmacological approach. Here we addressed the influence of PARP on the hemodynamic alterations and the survival of HS. In addition, we defined the role of PARP in alterations that are considered pivotal events in the pathophysiology of HS, namely, gut mucosal barrier failure and lung inflammation. Our results provide evidence that PARP activation takes place early in resuscitated HS and is an important mechanism contributing to multiple organ damage in this setting.

Materials and Methods

In vivo studies were performed in accordance with National Institutes of Health guidelines and with the approval of the local institutional animal care and use committee.

Surgical Procedure. Colonies of $PARP^{-/-}$ and wild-type $PARP^{+/+}$ mice originally derived from Dr. Z. Q. Wang's laboratory (Institute of Molecular Pathology, Vienna) were maintained and bred in our animal facility. Male mice (age, 8–10 weeks; weight, 24–28 g) were anesthetized with i.p. injections of ketamine (80 mg/kg) and xylazine (10 mg/kg). The right carotid artery was cannulated with polyethylene tubing (PE-10) and connected to a pressure transducer (World Precision Instruments, Sarasota, FL) for blood pressure (BP) measurements. Pressure signals were recorded by using a MacLab A/D converter (A. D. Instruments, Mountain View, CA) A. D. and continuously displayed on a MacIntosh computer. The right

This paper was submitted directly (Track II) to the PNAS office.

Abbreviations: PARP, poly(ADP-ribose) polymerase; HS, hemorrhagic shock; KHBB, Krebs–Henseleit bicarbonate buffer; FD4, FITC-conjugated dextran; MPO, myeloperoxidase; MDA, malondialdehyde; GSH, glutathione; BP, blood pressure; PAR, poly(ADP-ribose); PMN, polymorphonuclear.

†On leave from the Critical Care Division, Department of Internal Medicine, University Hospital, Lausanne, Switzerland.

§On leave from the Department of Critical Care Medicine, Hospital das Clinicas da Universidade de Sao Paulo, Brazil.

‖To whom reprint requests should be addressed. E-mail: szabocsaba@aol.com.

The publication costs of this article were defrayed in part by page charge payment. This article must therefore be hereby marked "*advertisement*" in accordance with 18 U.S.C. §1734 solely to indicate this fact.

Article published online before print: *Proc. Natl. Acad. Sci. USA*, 10.1073/pnas.170226797. Article and publication date are at www.pnas.org/cgi/doi/10.1073/pnas.170226797

femoral artery was cannulated with PE-10 tubing for blood withdrawal and administration of the resuscitation fluid.

HS Model. After surgery, the hemodynamic variables were allowed to stabilize for 20 min, after which the baseline hemodynamic values were recorded. Mice were then subjected to a severe HS by withdrawing blood from the femoral artery into a heparinized syringe over 30 min, at a rate of 0.5–1 μl/g/min to reach a mean BP of 45 mmHg. The volume of blood withdrawn was not different between individual groups (see *Results*). Animals were then monitored for 45 min. Additional blood withdrawal or restitution of small volumes of blood was performed to maintain mean BP at 45 mmHg during this period. After 45 min, the animals were resuscitated with a crystalloid solution (sterile isotonic saline), at a volume equal to two times the total amount of shed blood, infused through the femoral artery catheter over 10 min.

Experimental Protocols. In a first set of studies (Protocol 1), the time course of BP, as well as survival were analyzed in five $PARP^{-/-}$ and five $PARP^{+/+}$ mice. After resuscitation, BP was recorded until the death of the animal. In a second set of experiments (Protocol 2), mechanisms relevant to the pathophysiology of HS were investigated. These experiments were conducted in eight $PARP^{-/-}$ and eight $PARP^{+/+}$ mice subjected to HS as well as in five $PARP^{-/-}$ and five $PARP^{+/+}$ mice subjected to sham shock. The animals were killed at 30 min after the beginning of resuscitation (or sham resuscitation) by exsanguination, immediately followed by a midline laparotomy to harvest a 5-cm length of distal ileum for permeability studies (see below) and a thoracotomy to allow excision of the aorta for vascular ring studies (see below). Samples from the gut, liver, and lung were also harvested, snap frozen in liquid nitrogen, and stored at −70°C for further biochemical measurements, as detailed below. Blood was centrifuged and plasma stored at −70°C until assayed for the levels of nitrate/nitrite and IL-6 (see below).

Specific Measurements. *Gut permeability measurements.* Intestinal mucosal barrier function was assessed by the mucosal-to-serosal clearance of FITC-conjugated dextran (4 kDa; FD4) in everted gut ileal sacs incubated *ex vivo*, as described (7, 14). The everted gut sacs were prepared in ice-cold modified Krebs–Henseleit bicarbonate buffer (KHBB) at 10 mM Hepes/137 mM NaCl/5.5 mM KCl/4.2 mM $NaHCO_3$/0.3 mM Na_2HPO_4/0.4 mM KH_2PO_4/0.4 mM $MgSO_4$/0.5 mM $MgCl_2$/1.3 mM $CaCl_2$/19.5 mM glucose/pH 7.4. The ileal segment was first lavaged with 3 ml of isotonic saline to remove fecal material and was then closed at one end with a 4-0 silk ligature. The gut sac was everted onto a thin plastic rod, then connected to a 3-ml syringe containing 0.4 ml of the KHBB solution, via a male luer fitting for ≈1.5-mm internal diameter tubing (World Precision Instruments), and secured with a 4-0 silk ligature. The everted gut sac was then gently distended with 0.4 ml of KHBB and then suspended in a 50-ml beaker containing 40 ml of a solution of FD4 (20 μg/ml) in KHBB, continuously bubbled with 95% O_2 and 5% CO_2 and maintained at 37°C in a water bath.

At the beginning of the incubation, a 1-ml sample was withdrawn from the beaker to determine the initial external (i.e., mucosal) FD4 concentration ($FD4_{muc}$). After a 30-min incubation period, the gut sac was removed from the beaker; its diameter (D) and length (L) measured; and the KHBB solution (0.4 ml) was withdrawn from within the sac to determine the internal (i.e., serosal) FD4 concentration ($FD4_{ser}$). After centrifugation (1,000 × g for 10 min), 300 μl of the clear supernatants was diluted with 3 ml of PBS (10 mM, pH 7.4), and fluorescence was measured (λ_{ex} = 492 nm; slit width = 1.5 nm; λ_{em} = 515 nm; slit width = 10 nm) in a spectrofluorometer (model RF 5301, Shimadzu, Columbia, MD). The mucosal-to-serosal clearance of FD4 (C) was calculated by using the following equation: $C(nL/\text{min}/\text{cm}^2) = FD4_{ser} \times 0.4 \times 30^{-1} FD4_{muc}{}^{-1} \times (\pi LD)^{-1}$.

Measurement of Vascular Reactivity in Isolated Aortic Rings. The thoracic aorta was cleared from periadventitial fat and cut into 0.5- to 1-mm width rings, mounted in organ baths filled with warmed (37°C) and oxygenated (95% O_2, 5% CO_2) Krebs solution (1.6 mM $CaCl_2$/1.17 mM $MgSO_4$/0.026 mM EDTA/130 mM NaCl/14.9 mM $NaHCO_3$/4.7 mM KCl/1.18 mM KH_2PO_4/11 mM glucose). Isometric forces were measured with isometric transducers (Kent Scientific Corporation, Litchfield, CT), digitized by using a MacLab A/D converter, and stored and displayed on a Macintosh computer. A tension of 1 g was applied, and the rings were equilibrated for 60 min, followed by measurements of the concentration-dependent contraction to prostaglandin F2α (10^{-10} to 3 × 10^{-6} M) and relaxation to acetylcholine (10^{-9} to 10^{-5} M). These experiments were conducted in five pairs of rings in each experimental group.

Biochemical Measurements. *Myeloperoxidase (MPO) assay.* Tissues were homogenized (50 mg/ml) in 0.5% hexadecyltrimethylammonium bromide in 10 mM 3-(*N*-morpholino)propanesulfonic acid (Mops) and centrifuged at 15,000 × g for 40 min. The suspension was then sonicated three times for 30 s. An aliquot of supernatant was mixed with a solution of 1.6 mM tetramethylbenzidine and 1 mM hydrogen peroxide. Activity was measured spectrophotometrically as the change in absorbance at 650 nm at 37°C by using a Spectramax microplate reader (Molecular Devices). Results are expressed as milliunits MPO activity per milligram of protein, which were determined with the Bio-Rad assay.

Malondialdehyde (MDA) assay. MDA formation was used to quantify the lipid peroxidation in tissues and measured as thiobarbituric acid-reactive material. Tissues were homogenized (100 mg/ml) in 1.15% KCl buffer. Homogenates (200 μl) were then added to a reaction mixture consisting of 1.5 ml of 0.8% thiobarbituric acid, 200 μl of 8.1% (vol/vol) SDS, 1.5 ml of 20% (vol/vol) acetic acid (pH 3.5), and 600 μl of distilled H_2O and heated at 90°C for 45 min. After cooling to room temperature, the samples were cleared by centrifugation (10,000 × g for 10 min), and their absorbance was measured at 532 nm by using 1,1,3,3-tetramethoxypropane as an external standard. The level of lipid peroxides was expressed as nanomoles MDA per milligram of protein.

Glutathione (GSH) assay. Tissues were homogenized (100 mg/ml) in 5% (vol/vol) sulfosalicylic acid. The homogenates were centrifuged at 10,000 × g for 20 min, and an aliquot of the clear supernatant (20 μl) was combined with 0.3 M Na_2HPO_4 (160 μl) and 0.04% 5,5′-dithiobis-(2-nitrobenzoic acid) in 1% sodium citrate (20 μl). After a 10-min incubation at room temperature, absorbance was read at 405 nm in a Spectramax microplate reader. Concentrations of GSH were calculated from a standard curve constructed with known concentrations of reduced GSH.

Plasma nitrate and nitrite. Plasma nitrate/nitrite, an index of NO production, was measured by the Griess method as described (15).

Plasma levels of IL-6. Plasma levels of IL-6 were determined by a commercially available ELISA (R & D Systems) according to the manufacturer's protocol.

Immunohistochemical detection of PAR and nitrotyrosine. Paraffin sections (3 μm) were deparaffinized in xylene and rehydrated in decreasing concentrations (100, 95, and 75%) of ethanol followed by a 10-min incubation in PBS (pH 7.4). Sections were treated with 0.3% hydrogen peroxide for 15 min to block endogenous peroxidase activity and then rinsed briefly in PBS. Nonspecific binding was blocked by incubating the slides for 1 h in PBS containing 2% (vol/vol) horse serum. To detect PAR, a routine histochemical procedure was applied as described (16) with minor modifications, as follows. Mouse monoclonal anti-poly(ADP-ribose) antibody (Alexis, San Diego) and isotype-matched control antibody was applied in a dilution of 1:100 for 2 h at room temperature. After

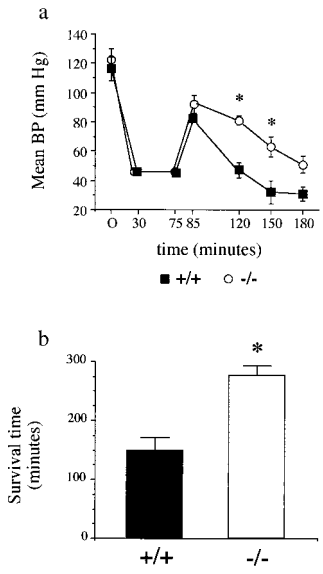

Fig. 1. Time course of mean BP (*a*) and mean survival time (*b*) in mice subjected to HS and resuscitation (Protocol 1). Mice (five $PARP^{+/+}$ and five $PARP^{-/-}$) were bled over 30 min to a mean BP of 45 mmHg. This mean BP was maintained for 45 min, followed by resuscitation with isotonic saline (administered over 10 min) at a volume of 2× the shed blood volume. Mice were then observed until death, and the overall survival time was recorded. Values are shown as means ± SEM. *, $P < 0.05$ $PARP^{-/-}$ vs. $PARP^{+/+}$ mice.

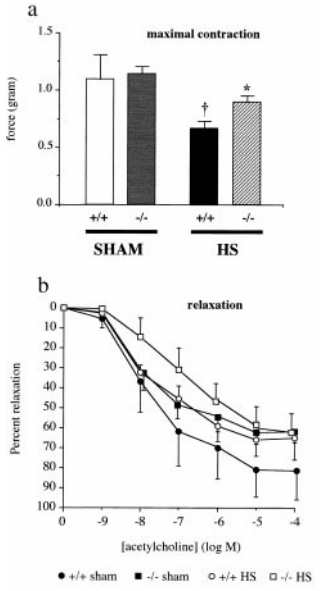

Fig. 2. Vascular ring experiments. Mice were bled over 30 min to a mean BP of 45 mmHg. This BP was then maintained for 45 min, followed by resuscitation with isotonic saline (administered over 10 min), at a volume of 2× the shed blood volume. Thoracic aortae ($n = 5$ per group) were harvested 30 min after the beginning of resuscitation to measure their contraction to prostaglandin F2α (*a*) and relaxation to acetylcholine (*b*) *ex vivo*. The respective IC_{50} values for relaxant responses to acetylcholine were $5.4 \pm 5.3 \times 10^{-7}$ M; $1.4 \pm 0.5 \times 10^{-8}$ M; $6.1 \pm 4.3 \times 10^{-8}$ M, and $2.8 \pm 1.3 \times 10^{-7}$ M in the $PARP^{+/+}$ sham, $PARP^{+/+}$ shocked, $PARP^{-/-}$ sham, and $PARP^{-/-}$ shocked groups, respectively, and there was no statistically significant difference between these values. Experiments were conducted in five $PARP^{+/+}$ and five $PARP^{-/-}$ mice exposed to sham shock. Values are shown as means ± SEM. †, $P < 0.05$ vs. sham mice; *, $P < 0.05$ $PARP^{-/-}$ vs. $PARP^{+/+}$ mice.

extensive washing (five times for 5 min) with PBS, immunoreactivity was detected with a biotinylated goat anti-rabbit secondary antibody and the avidin-biotin-peroxidase complex both supplied in the Vector Elite kit (Vector Laboratories). Color was developed by using Ni-DAB substrate (95 mg diaminobenzidine/1.6 g NaCl/2 g nickel sulfate in 200 ml of 0.1 M acetate buffer). Sections were then counterstained with nuclear fast red, dehydrated, and mounted in Permount. Photomicrographs were taken with a Zeiss Axiolab microscope equipped with a Fuji HC-300C digital camera. Detection of nitrotyrosine, a marker of peroxynitrite formation, was performed as described for PAR staining except that rabbit anti-nitrotyrosine polyclonal antibody was used as primary antibody.

Reagents. All reagents were obtained from Sigma unless indicated otherwise.

Statistical Analysis. All data are presented as means ± SEM. In the vascular rings experiments, differences between groups were analyzed by the unpaired *t* test. All of the other variables were analyzed by using ANOVA. When the relevant *F* values were significant at the 5% level, further pairwise comparisons were made by using Tukey's test for multiple comparisons. Statistical significance was assigned to $P < 0.05$.

Results

BP and Survival Times. The time course of mean BP (mean BP) is illustrated in Fig. 1*a*. At the end of the 30-min hemorrhage period, mean BP was 46 ± 1 mmHg in $PARP^{-/-}$ and 46 ± 2 mm Hg in $PARP^{+/+}$ mice and was maintained at the same levels during the next 45 min. The shed blood volume to reach and maintain the targeted BP was not different between groups both at 30 (22.7 ± 1.5 ml/kg vs. 22.9 ± 2.1 ml/kg in $PARP^{-/-}$ and $PARP^{+/+}$ mice, respectively) and 75 min (25.4 ± 1.6 vs. 24.1 ± 2.8 ml/kg). At the end of resuscitation, both groups experienced a comparable increase in mean BP, which nevertheless did not reach the baseline values. After resuscitation, a rapid decrease in mean BP was observed in $PARP^{+/+}$ mice. This decrease in BP was significantly attenuated in $PARP^{-/-}$ animals. Statistical analysis could no longer be done at the 180-min time point because of the fact that only two surviving $PARP^{+/+}$ mice could be included.

Fig. 1*b* shows the mean survival times recorded for both groups of mice. Death occurred significantly earlier in the $PARP^{+/+}$ mice, whose mean survival time was 149 ± 23 min, in contrast with 277 ± 16 min in $PARP^{-/-}$ animals.

Vascular Rings Experiments. The results of the vascular studies are shown in Fig. 2. The maximal contraction of aortic rings to prostaglandin F2α was significantly reduced in $PARP^{+/+}$ mice at 30 min after the beginning of resuscitation, an abnormality that did not occur in $PARP^{-/-}$ mice subjected to HS, as depicted in Fig. 2*a*. Interestingly, the rings of the $PARP^{-/-}$ mice responded to acetylcholine to a lesser degree of relaxation, although the difference failed to reach statistical significance (Fig. 2*b*). The mechanism of this phenotypic difference between $PARP^{+/+}$ and $PARP^{-/-}$ mice still needs to be explored.

After HS, the maximal relaxation to acetylcholine in the $PARP^{+/+}$ mice (but not the $PARP^{-/-}$ mice) tended to diminish, although the difference was not statistically significant. There were no statistically significant differences in between the four groups of rings in terms of sensitivity to acetylcholine, as judged by the respective IC_{50} values (Fig. 2*b*).

Plasma Levels of Nitrate/Nitrite and IL-6. Except from slight, nonsignificant variations between the four groups of animals studied, there was no difference in the plasma levels of nitrate/nitrite, indicating that NO production was not upregulated after 105 min of HS and resuscitation in our study (data not shown). There was a marked increase in animals exposed to HS and resuscitation compared with sham animals.

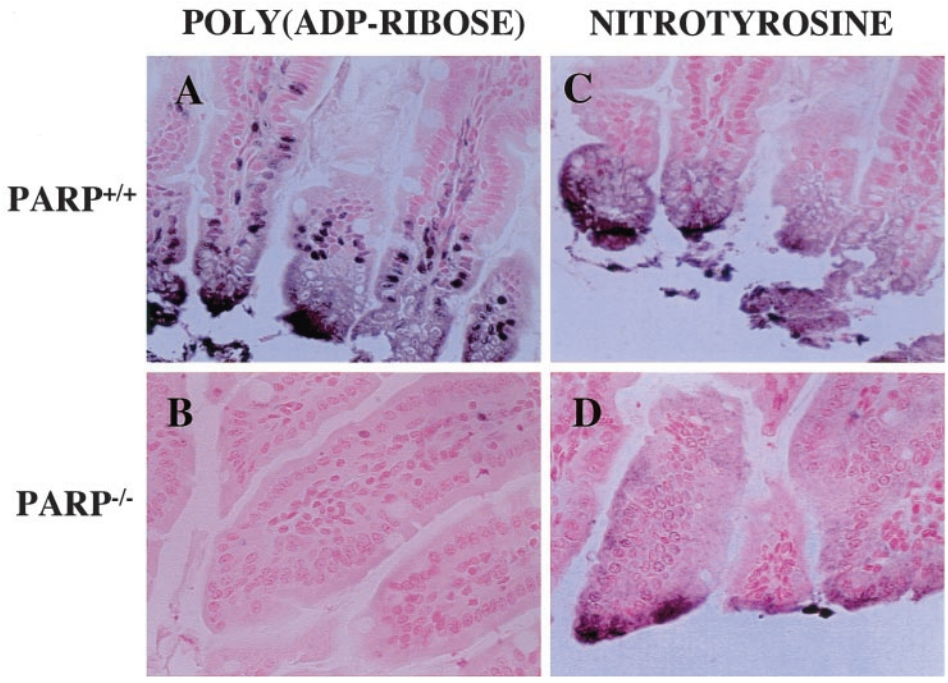

Fig. 3. Immunohistochemical detection of PAR and nitrotyrosine in the gut of mice subjected to HS and resuscitation. Guts were removed from PARP$^{+/+}$ (*A* and *C*) and PARP$^{-/-}$ (*B* and *D*) mice after HS and resuscitation, and tissue sections were stained for PAR as described in *Materials and Methods*. PAR and nitrotyrosine have been detected in the epithelial cells with strongest immunopositivity at the tip of the villi. Several stromal cells also displayed PAR positivity. No immunopositivity for PAR, reduced nitrotyrosine staining, and markedly maintained intestinal morphology were detected in the gut of, PARP$^{-/-}$ mice (*B* and *D*). (Magnification ×400.)

The increase in IL-6 was not statistically significantly different between PARP$^{+/+}$ and PARP$^{-/-}$ mice. Plasma IL-6 levels increased from 196 ± 17 to 1,123 ± 234 pmol/ml in wild-type animals and from 204 ± 21 to 1,089 ± 214 pmol/ml in the animals lacking PARP (n = 6).

PAR Polymerase Activation and Nitrotyrosine Formation. In the gut of mice subjected to HS and resuscitation, we have detected by immunohistochemistry the formation of PAR as an indicator of *in vivo* PARP activation (Fig. 3). PAR staining was most intense at the damaged tip of the villi, and localized in the necrotic epithelial cells. Furthermore, nuclei of intestinal epithelial cells and stromal cells also displayed strong immunostaining for PAR (Fig. 3*A*). In contrast, no PAR staining was detected in the gut of PARP$^{-/-}$ mice subjected to HS and resuscitation (Fig. 3*B*). There was also a significant degree of tyrosine nitration in the guts of animals subjected to HS, the majority of which colocalized with PAR staining to the tips of the injured villi (Fig. 3*C*). Nitrotyrosine staining was also found in the gut of the PARP$^{-/-}$ mice, again, mostly localizing to the tip of the villi (Fig. 3*D*).

Gut Mucosal Barrier Selectivity. The mucosal-to-serosal passage of FD4 was low in sham-shocked animals, the calculated clearance being 22.4 ± 4.1 and 26.2 ± 3.4 nl/min/cm^2 in PARP$^{+/+}$ and PARP$^{-/-}$ mice, respectively (Fig. 4). In line with the massive PARP activation, as visualized with immunohistochemistry, HS and resuscitation induced a sharp increase in gut permeability in PARP$^{+/+}$ mice, the calculated clearance reaching 90.5 ± 17.4 nl/min/cm^2. In contrast, the clearance calculated in PARP$^{-/-}$ mice was significantly lower (39.9 ± 5.9 nl/min/cm^2) and was not significantly different from that of the sham animals (Fig. 4).

Tissue MPO. In the gut and liver, MPO activities were comparable in all groups of mice (Fig. 5), indicating that, at the time point chosen for this study, polymorphonuclear (PMN) infiltration was not a prevalent feature of HS and resuscitation in these organs. A clearly different pattern was noted in the lungs, where the activity of MPO showed a marked increase in PARP$^{+/+}$ mice subjected to HS and resuscitation, whereas PARP$^{-/-}$ animals were protected from this early PMN infiltration.

Tissue Levels of MDA and Reduced GSH. We did not notice any significant alterations in the levels of MDA in the lungs and guts of sham-shocked or HS and resuscitation animals (not shown). However, in the liver, MDA generation was significantly enhanced in PARP$^{+/+}$ mice subjected to HS and resuscitation (from 0.71 ± 0.19 to 1.53 ± 0.32 nmol/mg protein; $P < 0.01$, n = 6). In PARP$^{-/-}$ mice, however, no statistically significant increase was found, when compared with the value measured in sham mice. The GSH content of the gut and liver has also been determined, and no significant differences have been observed between PARP$^{+/+}$ and PARP$^{-/-}$ tissues (not shown).

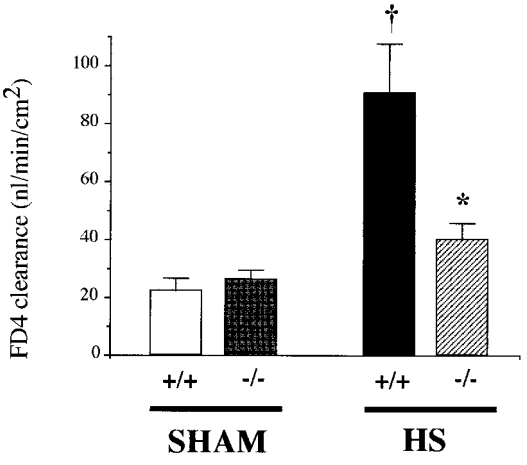

Fig. 4. Gut mucosal permeability to FD4 in everted gut sacs incubated *ex vivo*. Mice (eight PARP$^{+/+}$ and eight PARP$^{-/-}$) were bled over 30 min to a mean BP of 45 mmHg. This BP was then maintained for 45 min, followed by resuscitation with isotonic saline (administered over 10 min) at a volume of 2× the shed blood volume. A segment of ileum was harvested 30 min after the beginning of resuscitation to measure the mucosal-to-serosal passage of FD4. The same experiments were made in five PARP$^{+/+}$ and five PARP$^{-/-}$ mice exposed to sham shock. Values are shown as means ± SEM. †, $P < 0.05$ vs. sham mice; *, $P < 0.05$ PARP$^{-/-}$ vs. PARP$^{+/+}$ mice.

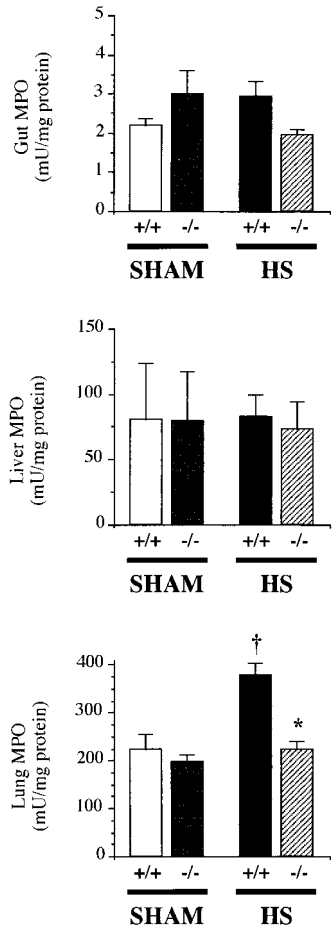

Fig. 5. MPO activity in the gut (*Top*), liver (*Middle*), and lung (*Bottom*). Tissues were harvested from mice exposed to HS and resuscitation (eight $PARP^{+/+}$ and eight $PARP^{-/-}$) or sham shock (five $PARP^{+/+}$ and five $PARP^{-/-}$) 30 min after the beginning of resuscitation (or sham resuscitation), after a 45-min period of HS (or sham shock). Values are shown as means ± SEM. †, $P < 0.05$ vs. sham mice; *, $P < 0.05$ $PARP^{-/-}$ vs. $PARP^{+/+}$ mice.

Discussion

We demonstrated that targeted disruption of the PARP gene significantly reduced the consequences of HS and resuscitation in the mouse. $PARP^{-/-}$ animals were protected from the rapid cardiovascular decompensation developing soon after resuscitation and showed a clear survival advantage in comparison to wild-type littermates. Furthermore, the pathophysiological alterations occurring in early reperfusion, notably vascular hypocontractility, gut barrier failure, and lung neutrophil recruitment, were suppressed in the PARP knockout phenotype. Furthermore, we have provided direct evidence for PARP activation in the necrotic intestinal epithelial and stromal cells of mice subjected to HS.

Role of PARP in the Cardiovascular Failure of HS. Resuscitation was followed by a rapid decline in BP in $PARP^{+/+}$ mice (Fig. 1*a*), leading to death in less than 3 h. In contrast, the fall in BP was significantly blunted, and survival was significantly prolonged in $PARP^{-/-}$ animals. The reduced hypotension observed in $PARP^{-/-}$ mice was related, at least partially, to an improved vascular reactivity to vasoconstrictors. Although it has been shown that an enhanced formation of NO, caused by the expression of inducible NO synthase, contributes to the delayed cardiovascular failure in HS (17), it is unlikely that this was a prevailing mechanism in the relatively short-term experiments of our study. Indeed, we did not find any increase in plasma nitrate/nitrite, the stable metabolites of NO in blood, at times when already significant hemodynamic and functional alterations were seen in the animals subjected to HS. Thus, the beneficial hemodynamic consequences of PARP suppression are probably not related to a modulation of NO production. Thus, our study places the role of PARP in the pathogenesis of HS to a point more proximal than previously expected.

Other possible mechanisms of vascular failure, including activation of ATP-sensitive K^+ channels, or the generation of vasodilating prostaglandins cannot be ruled out but seem also unlikely in light of a recent report showing that these pathways were not causally associated with the early vascular failure complicating HS (18). Our group has demonstrated that the production of peroxynitrite (an important trigger of PARP activation in pathophysiological conditions) precedes the expression of the inducible isoform of NOS in HS and is related to the reaction of superoxide and NO produced from constitutive isoforms of NOS (10). We propose, therefore, that this early generation of peroxynitrite (in combination with hydroxyl radicals, which are known to be produced in HS and which are capable of inducing DNA strand breakage and PARP activation) leads to PARP activation in the vascular smooth muscle. The salutary effect of PARP suppression on vascular function can, therefore, be related to an improved energetic status of the smooth vascular muscle cells. In this respect, it should be mentioned that activation of PARP leading to cellular energy depletion has been demonstrated in smooth muscle cells exposed to peroxynitrite (19).

In contrast to the depressed vascular contractility, we did not find any significant reduction in the relaxation elicited by acetylcholine. This observation, which agrees with similar reported findings (20), indicates that endothelial function was well maintained at the relatively early stage (30 min) of resuscitation in our model.

Role of PARP in the Multiple Organ Damage Associated with HS. A number of studies have highlighted the central role of the gut in the pathophysiology of shock of various etiologies, notably HS. The gut is particularly prone to develop both ischemic and reperfusion injuries caused by the countercurrent shunting of blood in the villi (21), as well as the abundant content of xanthine dehydrogenase/xanthine oxidase in the gut mucosa (22). In addition, mesenteric perfusion remains severely jeopardized despite the restoration of central hemodynamics in resuscitated HS (23).

Here we provided evidence that HS and resuscitation induces PARP activation in the intestinal epithelial cells as well as in the intestinal stromal cells, and it localized to the areas of epithelial cell injury (i.e., the tip of the villi, which are most sensitive to ischemic insults and injury). Moreover, we found that $PARP^{+/+}$ animals subjected to HS developed a significant gut mucosal barrier failure, as evidenced by a marked increase in gut permeability to FD4. In sharp contrast, $PARP^{-/-}$ mice did not exhibit any significant increase in intestinal permeability when compared with sham-operated animals, implying that PARP activation plays an important mechanistic role in the development of HS-induced gut dysfunction. The immunohistochemical findings presented in Fig. 3 show a significant colocalization of nitrotyrosine and PAR, supporting the hypothesis that reactive nitrogen species such as peroxynitrite are involved in the activation of PARP.

Of note, we recently reported a similar protection against intestinal hyperpermeability in $PARP^{-/-}$ mice exposed to mesenteric ischemia-reperfusion injury (7), supporting the concept that PARP is a common effector of intestinal damage in various forms of shock and trauma. Recent data have indicated that HS results in a decrease in gut ATP content, which is directly correlated to the severity of mucosal barrier failure (24). Because ATP depletion is a major consequence of PARP activation (4), it is therefore reasonable to assume that the suppression of gut dysfunction is related to an improvement of the energy status of the gut mucosa. In fact, in our recent *in vitro* studies, we have demonstrated that the

peroxynitrite-induced intestinal hyperpermeability is, at least in part, related to PARP activation (25). The mode of inhibition by inhibition of PARP is most likely related to suppression of oxidant-induced cell necrosis (3, 4, 25).

It is noteworthy that the degree of tyrosine nitration was reduced in the gut of the $PARP^{-/-}$ mice, when compared with the response seen in $PARP^{+/+}$ animals. This difference may be related either to interruption of positive feedback cycles of tissue injury in the absence of functional PARP, or alternatively, to a reduced net cellular oxidant generation by the epithelial cells in HS. In fact, our recent *in vitro* finding, demonstrating a reduced degree of time-dependent mitochondrial oxidant generation in $PARP^{-/-}$ thymocytes challenged with peroxynitrite, when compared with $PARP^{+/+}$ cells (26), favors the latter possibility.

It is worth noting that we did not find any reduction of tissue GSH level, nor could we detect any increase in MDA formation, an index of lipid peroxidation, in the gut of HS mice. In addition, in agreement with data obtained by other investigators (27), we did not notice any increase in MPO in the gut (Fig. 5), which makes the formation of oxyradicals from recruited neutrophils unlikely in the intestine of HS animals. Similar observations were made in the liver, with the exception of a slight but significant increase in MDA formation in $PARP^{+/+}$ mice, which was reduced in $PARP^{-/-}$ mice. Overall, from these findings, the following possibilities may be considered. The first option is that the oxidant stress and the subsequent activation of PARP are tightly localized to a small fraction of cells (for example, the epithelial cells at the tip of the villi), which does not therefore result in alterations in the net GSH and MDA values in whole-tissue homogenates. This option is favored by the fact that nitrotyrosine staining was also found tightly localized to relatively small areas at the tips of the villi. The second possibility is that the generation of oxidant species and free radicals remained limited at this stage of HS and that the antioxidant defense system was not jeopardized, at least at 30 min after resuscitation in our model. The salutary effect of genetic disruption of PARP on gut function would indicate, therefore, that PARP activation takes place well before the bulk formation of oxidants, thus being a highly sensitive, relatively early effector mechanism of reperfusion injury. The third possibility, that the activator of PARS in the early stage of HS is a stimulus other than oxidant stress, can also be considered. A fourth possibility, namely, that the currently used GSH and MDA assays have low sensitivity, can be excluded, based on the finding that, by using the same assays, we have observed massive changes in the gut in these parameters in a splanchnic occlusion model (28) and in endotoxic shock (L.L. and C.S., unpublished data).

An additional feature of our study was the rapid accumulation of PMN in the lung (assessed by the activity of MPO) of $PARP^{+/+}$ mice, whereas $PARP^{-/-}$ animals were protected from this abnormality. Such recruitment of lung PMN in HS has been ascribed to the rapid up-regulation of adhesion molecules, most significantly *P*-selectin and intercellular adhesion molecule-1, on vascular pulmonary endothelial cells (29). It is noteworthy at this point that previous data from our group have shown that genetic inactivation of PARP was associated with a down-regulation of selectin expression in models of localized ischemia-reperfusion (30), by a yet undetermined mechanism. Such interaction may also have occurred in the present study. In addition, it has been proposed that PMN activation ("priming"), followed by their recruitment in various organs, notably the lung, was triggered by factors contained in mesenteric lymph (31–33), suggesting a critical link between gut dysfunction, PMN activation, and distant organ injury in HS. The suppression of lung PMN recruitment in $PARP^{-/-}$ mice is consistent with this hypothesis, in view of the marked protection against gut barrier failure in these animals.

Finally, lung inflammation complicating the course of HS has also been associated with the up-regulation of IL-6 production, a cytokine considered as central in the pathophysiology of HS (34, 35). In particular, IL-6 is important for PMN recruitment in tissues, by inducing IL-8, a C-X-C chemokine (36). Here, we found that plasma IL-6 rapidly increased on resuscitation, confirming that it is a very proximal component of the acute phase response in this setting. It is noteworthy that this increase was similar in both $PARP^{+/+}$ and $PARP^{-/-}$ animals, evidencing that the beneficial effects of PARP suppression, notably on lung PMN recruitment, were not related to a modulation of signaling through IL-6. Also, this observation indicates that factors independent from IL-6 modulate PMN accumulation in the lungs during resuscitated HS.

Conclusions

Activation of PARP is increasingly recognized as a common pathway of tissue damage in conditions associated with the formation of oxidant species and free radicals. In the present study, we provide definitive proof (*i*) that PARP is activated in HS; (*ii*) that its activation is an early pathophysiological process that localizes to areas of the injury; and (*iii*) that PARP activation is a critical factor mediating cardiovascular failure, gut dysfunction, lung inflammation, and death in HS. It is clear from the clinical experience that fluid resuscitation alone is not sufficient to prevent mortality or multiple organ failure in patients with HS. Fluid resuscitation, combined with pharmacological blockade of PARP, may be an effective concept for the therapy of HS.

This study was supported in part by National Institutes of Health Grants R29 GM 54773 and RO1 GM 60915 (to C.S.). F.G.S. is supported by a fellowship from Fundacao de Amparo à Pesquisa do Estado de Sao Paulo (Brazil).

1. Angele, M. K., Schwacha, M. G., Smail, N., Catania, R. A., Ayala, A., Cioffi, W. G. & Chaudry, I. H. (1999) *Am. J. Physiol.* **276,** C285–C290.
2. Szabo, C. & Dawson, V. L. (1998) *Trends Pharmacol. Sci.* **19,** 287–298.
3. Virag, L., Scott, G. S., Cuzzocrea, S., Marmer, D., Salzman, A. L. & Szabo, C. (1998) *Immunology* **94,** 345–355.
4. Ha, H. C. & Snyder, S. H. (1999) *Proc. Natl. Acad. Sci. USA* **96,** 13978–13982.
5. Liaudet, L., Garcia-Soriano, F. & Szabo, C. (2000) *Crit. Care Med.* **28,** N37–N52.
6. Yang, Z., Zingarelli, B. & Szabo, C. (2000) *Shock* **13,** 60–66.
7. Liaudet, L., Szabo, A., Garcia-Soriano, F., Zingarelli, B., Szabo, C. & Salzman, A. L. (2000) *Shock*, in press.
8. Szabo, C., Wong, H., Bauer, P., Kirsten, E., O'Connor, M., Zingarelli, B., Mendeleyev, J., Hasko, G., Vizi, E., Salzman, A., *et al.* (1997) *Int. J. Oncol.* 1093–1101.
9. Szabo, C., Zingarelli, B. & Salzman, A. L. (1996) *Circ. Res.* **78,** 1051–1063.
10. Szabo, C., Salzman, A. L. & Ischiropoulos, H. (1995) *FEBS Lett.* **372,** 229–232.
11. Lazarus, H. M., Warnick, C. T. & Hutto, W. (1984) *Circ. Shock* **13,** 171–181.
12. McDonald, M. C., Filipe, H. M. & Thiemermann, C. (1999) *Br. J. Pharmacol.* **128,** 1339–1345.
13. Szabo, A., Hake, P., Salzman, A. L. & Szabo, C. (1998) *Shock* **10,** 347–353.
14. Wattanasirichaigoon, S., Menconi, M. J., Delude, R. L. & Fink, M. P. (1999) *Shock* **11,** 269–275.
15. Szabo, C., Zingarelli, B. & Salzman, A. L. (1996) *Circ. Res.* **78,** 1051–1063.
16. Scott, G. S., Jakeman, L. B., Stokes, B. T. & Szabo, C. (1999) *Ann. Neurol.* **45,** 120–124.
17. Szabo, C. & Billiar, T. R. (1999) *Shock* **12,** 1–9.
18. Pieber, D., Horina, G., Sandner-Kiesling, A., Pieber, T. R. & Heinemann, A. (1999) *Cardiovasc. Res.* **44,** 166–175.
19. Szabo, C., Zingarelli, B., O'Connor, M. & Salzman, A. L. (1996) *Proc. Natl. Acad. Sci. USA* **93,** 1753–1758.
20. Zingarelli, B., Ischiropoulos, H., Salzman, A. L. & Szabo, C. (1997) *Eur. J. Pharmacol.* **338,** 55–65.
21. Revelly, J. P., Ayuse, T., Brienza, N., Fessler, H. E. & Robotham, J. L. (1996) *Crit. Care Med.* **24,** 1345–1351.
22. Qu, X. W., Rozenfeld, R. A., Huang, W., Bulkley, G. B. & Hsueh, W. (1999) *Gut* **44,** 203–211.
23. Flynn, W. J., Jr., Pilati, D. & Hoover, E. L. (1997) *Shock* **8,** 300–304.
24. Wattanasirichaigoon, S., Menconi, M. J., Delude, R. L. & Fink, M. P. (1999) *Shock* **12,** 127–133.
25. Kennedy, M., Denenberg, A. G., Szabo, C. & Salzman, A. L. (1998) *Gastroenterology* **114,** 510–518.
26. Virág, L., Salzman, A. L. & Szabó, C. (1998) *J. Immunol.* **161,** 3753–3759.
27. Childs, E. W., Wood, J. G., Smalley, D. M., Hunter, F. A. & Cheung, L. Y. (1999) *Shock* **11,** 248–252.
28. Liaudet, L., Szabo, A., Soriano, F. G., Szabo, C. & Salzman, A. L. (2000) *Shock* **14,** 134–141.
29. Ramos-Kelly, J. R., Toledo-Pereyra, L. H., Jordan, J. A., Rivera-Chavez, F. A., Dixon, R. A. & Ward, P. A. (1999) *J. Am. Coll. Surg.* **189,** 546–553.
30. Zingarelli, B., Salzman, A. L. & Szabo, C. (1998) *Circ. Res.* **83,** 85–94.
31. Zallen, G., Moore, E. E., Johnson, J. L., Tamura, D. Y., Ciesla, D. J. & Silliman, C. C. (1999) *J. Surg. Res.* **83,** 83–88.
32. Zallen, G., Moore, E. E., Tamura, D. Y., Johnson, J. L., Biffl, W. L. & Silliman, C. C. (2000) *J. Trauma* **48,** 45–48.
33. Upperman, J. S., Deitch, E. A., Guo, W., Lu, Q. & Xu, D. (1998) *Shock* **10,** 407–414.
34. Hierholzer, C., Kalff, J. C., Omert, L., Tsukada, K., Loeffert, J. E., Watkins, S. C., Billiar, T. R. & Tweardy, D. J. (1998) *Am. J. Physiol.* **275,** L611–L621.
35. Hierholzer, C., Kalff, J. C., Bednarski, B., Memarzadeh, F., Kim, Y. M., Billiar, T. R. & Tweardy, D. J. (1999) *Arch. Orthop. Trauma Surg.* **119,** 332–336.
36. Romano, M., Sironi, M., Toniatti, C., Polentarutti, N., Fruscella, P., Ghezzi, P., Faggioni, R., Luini, W., van Hinsbergh, V., Sozzani, S., *et al.* (1997) *Immunity* **6,** 315–325.